Materials Today Bio 21 (2023) 100715

Contents lists available at ScienceDirect

Materials Today Bio

journal homepage: www.journals.elsevier.com/materials-today-bio

# An epigallocatechin gallate–amorphous calcium phosphate nanocomposite for caries prevention and demineralized enamel restoration

Danni Dai, Jianrong Wang, Hanshu Xie, Chao Zhang *

*Stomatological Hospital, School of Stomatology, Southern Medical University, Guangzhou 510280, China*

ARTICLE INFO

*Keywords:*
Epigallocatechin gallate
Enamel remineralization
Antibacterial activity
Dental caries

ABSTRACT

Biomineralization with amorphous calcium phosphate (ACP) is a highly effective strategy for caries prevention and defect restoration. The identification and interruption of cariogenic biofilm formation during remineralization remains a challenge in current practice. In this study, an epigallocatechin gallate (EGCG)-ACP functional nanocomposite was developed to prevent and restore demineralization by integrating the antibacterial property of EGCG and the remineralization effect of ACP. The synthesized EGCG-ACP showed good biocompatibility with L-929 cells and human gingival fibroblasts. Under neutral conditions, the sustained release of ACP from EGCG-ACP restored the microstructure and mechanical properties of demineralized enamel. Under acidic conditions, protonated EGCG released from EGCG-ACP exerted a strong antibacterial effect, and the ACP release rate doubled within 4 h, resulting in the prevention of demineralization in the presence of cariogenic bacteria. The pH-responsive features of EGCG-ACP to promote the protonation of EGCG and ACP release facilitated its performance in remineralization effect to overcome the difficulty of restoring demineralized enamel in a cariogenic acidic environment, which was evidenced by the in vivo experiment carried out in a rat oral cariogenic environment. The results of this study indicate the potential of EGCG-ACP for the prevention of enamel demineralization and provide a theoretical basis its application in populations with high caries risk.

## 1. Introduction

Dental caries are caused by acid etching from the acid production of cariogenic bacteria (e.g., *Streptococcus mutans*), fermentation of sucrose, exogenous acid intake, and gastric acid reflux. When the pH on the enamel surface decreases, hydrogen ions ($H^+$) attack hydroxyapatite (HA) and dissolve calcium (Ca) and phosphorous (P) components, which leads to demineralization and the resultant degradation of enamel morphology and impairment of its force-bearing function. More profoundly, caries may progress to dentin sensitivity and pulpitis, imposing considerable financial and quality-of-life burdens [1]. Mature enamel is an acellular, avascular, and highly mineralized tissue, which thus lacks the capacity for regenerative repair after damage [2]. Natural remineralization processes rely on salivary calcium ($Ca^{2+}$) and phosphate ($PO_4^{3-}$) ions, and are thereby insufficient. Thus, the development of new strategies to promote enamel remineralization is a significant but challenging issue in clinical efforts to prevent caries. The occurrence of enamel caries can be prevented to some extent by the reduction of sugar consumption and use of fluoride toothpaste. The key to preventing the occurrence and progression of dental caries is to inhibit cariogenic bacteria and promote remineralization.

Antibacterial drugs that have been used in the oral cavity (mainly chlorhexidine, metronidazole, roxithromycin, and clindamycin) affect the resident flora, disrupting the ecological balance and causing bacterial resistance [3,4]. In recent years, the application of natural antibacterial drugs has been explored. Epigallocatechin gallate (EGCG) is a polyphenolic substance with antibacterial, antioxidant, and anti-inflammatory activities, which has been shown to reduce bacterial virulence by inhibiting the expression of specific virulence factors and glucosyltransferase-related genes of *S. mutans* [5], as well as inhibiting bacterial proliferation [6]. EGCG has been used as an active component of treatments for cancer and infectious diseases, for the scavenging of free radicals and amelioration of inflammatory infiltration and oxidative stress [7–9]. It has not been applied widely in oral antibacterial therapy.

The mechanical performance of demineralized enamel is difficult to restore by simply inhibiting the proliferation of cariogenic bacteria, as HA regeneration requires $Ca^{2+}$ and $PO_4^{3-}$. Nanometer-scale, high-surface-area amorphous calcium phosphate (ACP) is the precursor of HA; it can

* Corresponding author.
*E-mail address:* 2645491781@qq.com (C. Zhang).

https://doi.org/10.1016/j.mtbio.2023.100715
Received 11 April 2023; Received in revised form 21 June 2023; Accepted 23 June 2023
Available online 24 June 2023

penetrate demineralized lesions rapidly to release high levels of $Ca^{2+}$ and $PO_4^{3-}$ for HA production [10]. The high reactivity makes ACP quick agglomerate and crystallize, thus difficult to be applied alone for effective remineralization [11]. Being loaded in drug delivery system or combined with other components may maintain its activity and facilitate its function [12]. Furthermore, the persistent cariogenic bacteria is a non-negligible obstacle for ACP to function, which limits its remineralization promotion capacity in acidic environments containing a mass of cariogenic bacteria with high caries risk. Thus, it is speculated that the combined use of EGCG and ACP may result simultaneously in an antibacterial effect and the promotion of $Ca^{2+}$ and $PO_4^{3-}$ infiltration and deposition on demineralized enamel, thereby preventing demineralization and promoting remineralization.

In this study, an EGCG-stabilized ACP nanocomposite (EGCG-ACP) with antibacterial and remineralization properties was prepared and characterized. The capability of this nanocomposite to inhibit *S. mutans* proliferation and biofilm development, and its effects on enamel demineralization and remineralization, were evaluated. ACP alone is extremely unstable and can spontaneously aggregate and even nucleate within a few seconds [13]. CPP-ACP is the only actually marketed formulation for enamel remineralization that is directly applied on the tooth surface [12,14]. Thus, the remineralization effect of EGCG-ACP was examined by comparing it to CPP-ACP. As for the remineralization effect of EGCG-ACP, we used demineralized enamel to investigate both in vitro and in vivo. As for the protective ability of EGCG-ACP on enamel, we examined it using sound enamel specimens. The results of this study support a novel direction of research on the early prevention of enamel demineralization and promotion of remineralization using nanocomposite materials, and provide the basis for the further application of natural antibacterial drugs in the prevention and treatment of dental caries.

## 2. Materials and methods

### 2.1. Materials

EGCG, calcium chloride dihydrate ($CaCl_2{\cdot}2H_2O$), and dipotassium hydrogen phosphate ($K_2HPO_4$) were purchased from Aladdin (Shanghai, China). CPP was purchased from Wako Pure Chemical Industries, Ltd (Japan). The cell counting kit-8 (CCK-8) was purchased from Dojindo Molecular Technologies (Japan). Dulbecco's modified Eagle's medium (DMEM), fetal bovine serum (FBS), Tris-buffered saline (TBS), and penicillin/streptomycin were obtained from Thermo Fisher Scientific (USA). Rhodamine (TRITC) phalloidin and 4′,6-diamidino-2-phenylindole (DAPI) were purchased from Solarbio Technology Ltd. (Beijing, China). Artificial saliva (ISO/TR10271) was obtained from Leagene Biotechnology (Anhui, China). Additional materials used in the cell-based experiments included 0.25% EDTA/trypsin (Gibco, USA), brain heart infusion (BHI) medium (Hopebiology, China), and the Cell Meter™ bacterial viability assay kit (AAT Bioquest Inc., USA).

### 2.2. Preparation of EGCG-ACP and CPP-ACP solution

EGCG-ACP was prepared as follows. EGCG (80 mg) and deionized water (10 mL) were mixed together to obtain a EGCG solution, and 11.76 mg $CaCl_2{\cdot}2H_2O$ was then added. $K_2HPO_4$ (8.352 mg) was dissolved in 30 mL deionized water, and the two solutions were mixed together with slight agitation to yield an EGCG-ACP solution (2 wt%). The obtained EGCG-ACP solution had 2 mM calcium ions and 1.2 mM phosphate ions, in which the molar ratio of $Ca^{2+}$ and $PO_4^{3-}$ was 5:3. The CPP-ACP solution was synthesized as previously described [15,16]. CPP (80 mg) was diluted in 10 mL deionized water to obtain a CPP solution, and 117.6 mg $CaCl_2{\cdot}2H_2O$ was then added. $K_2HPO_4$ (83.52 mg) was dissolved in 30 mL deionized water, and the two solutions were mixed with slight agitation to yield a CPP-ACP solution (2 wt%).

### 2.3. EGCG-ACP characterization

Dynamic light scattering (DLS) measurements were performed using a Zetasizer nano-ZS instrument (Malvern Instruments, Malvern, UK). The surface size and morphology of EGCG-ACP were characterized by transmission electron microscopy (TEM; Hitachi Ltd., Japan) at 110 kV, and the crystal structure was identified by selected-area electron diffraction (SAED). The elemental composition of EGCG-ACP was detected by X-ray photoelectron spectroscopy (XPS; Kratos, Japan). The typical functional groups of EGCG and EGCG-ACP were detected by Fourier-transform infrared spectroscopy (FTIR; Thermo Fisher Inc., USA).

To detect $Ca^{2+}$ release from the EGCG-ACP nanocomposite at different pHs, the pH of the solvent TBS (pH = 7.4) was adjusted with lactic acid. The detection timepoints were 1, 3, 5, and 7 days. At each timepoint, 1 mL supernatant was collected and the identical volume of fresh neutral or acidic TBS was supplemented. Ion exchange chromatography (ICS2500, Dionex FEI, USA) was used to detect $Ca^{2+}$ and $PO_4^{3-}$ release, and curves of this release were drawn.

### 2.4. Antibacterial and antibiofilm analyses

For a colony-forming unit (CFU) assay, *S. mutans* (ATCC25175) was inoculated in BHI agar medium at 37 °C for 48 h in an anaerobic environment to prepare a $10^8$ CFU/mL bacterial suspension. Deionized water and EGCG (2 wt%), casein phosphopeptide (CPP)-ACP (2 wt%), and EGCG-ACP (2 wt%) were co-incubated with the bacterial suspension for 24 h [17]. A 20-μL aliquot of the diluted solution ($10^{4-6}$ CFU/mL) was coated evenly on an agar plate and incubated anaerobically at 37 °C for 48 h.

The growth of *S. mutans* was examined by turbidimetry. One-milliliter aliquots of the bacterial suspension ($10^8$ CFU/mL) and the different test solutions were added to test tubes and incubated anaerobically at 37 °C for 0, 4, 8, 12, and 24 h [18]. A microplate reader (Molecular Devices, San Diego, CA, USA) was used to measure optical density at 600 nm ($OD_{600}$).

For an antibiofilm assay, 500 μL *S. mutans* ($10^8$ CFU/mL) was added to a 24-well plate containing sterile cell-climbing films and incubated for 24 h to form a biofilm. Varying solutions (500 μL) were added to the plate and co-cultured for 1 h. The attached bacteria were stained with a bacterial viability assay kit (AAT Bioquest Inc.) according to the recommended protocol. Fluorescent images of the biofilms were observed by confocal laser scanning microscopy (CLSM; FV1200, Olympus, Japan) and analyzed using the Image J software (National Institutes of Health, Bethesda, MD, USA).

### 2.5. Preparation of enamel specimens

The human enamel specimens for this study were prepared as reported previously [19]. Non-carious third molars were obtained from patients who underwent extractions at the Stomatological Hospital of Southern Medical University, Guangzhou, China (EC-CT-[2023]05). To obtain enamel samples (4 × 4 × 2 mm), the crowns were cut using a low-speed diamond saw. The samples were polished under flowing deionized water with silicon carbide papers (up to 5000 grit). The non-working sides were coated with acid-proof nail polish. All samples were sonicated for 30 min and then stored in 0.1% thymol solution.

### 2.6. Measurement of enamel remineralization without bacterial interference

For demineralized enamel preparation, the enamel samples were etched with 37% phosphoric acid, then rinsed and sonicated for 5 min to remove the residual crystals. Since ACP alone is extremely unstable, CPP-ACP was used to explore the remineralization effect of EGCG-ACP. The demineralized sample surfaces were coated with 100 μL deionized water,

and the EGCG, CPP-ACP, and EGCG-ACP solutions, then soaked in 5 mL sterile artificial saliva at 37 °C. This treatment was repeated every 12 h. In order to simulate a natural oral environment where the pH is essentially neutral, the remineralization effects of different solutions were mainly explored under neutral conditions. After treatment for 1, 3, 5, and 7 days, the samples were rinsed with deionized water and the extent of remineralization was characterized. Data were obtained from at least three independent experiments.

The surface morphology and elemental composition of the remineralized enamel were analyzed by scanning electron microscopy (SEM; Sigma 300, Zeiss, Germany) and energy dispersive spectroscopy (EDS; XFlash6I30, Bruker, Germany), respectively. The crystal orientation and mineral phase were analyzed by X-ray diffraction (XRD; Shimadzu Limited, Japan). Surface microhardness was measured using a Vicker's device (HXD-2000TM/LCD, Taiming, Shanghai, China), with the constant application of a 5-N load for 15 s and creation of 10 indentations per sample.

### 2.7. Examination of demineralization under acidic conditions created by cariogenic bacteria

Natural enamel samples were coated with deionized water and the EGCG, CPP-ACP, and EGCG-ACP solutions. Then, each sample was soaked in *S. mutans* bacterial solution ($10^8$ CFU/mL, pH ≈ 4) for 8 h, followed by ultraviolet sterilization and soaking in artificial saliva for 4 h at 37 °C. This cycle was repeated every 12 h to evaluate the tested solutions' protective effect against demineralization in the presence of cariogenic bacteria. After 1, 3, 5, and 7 days of treatment, the samples were rinsed with deionized water and changes in the enamel surface morphology, microhardness, calcium/phosphorus (Ca/P) ratio, and XRD pattern were examined.

### 2.8. Biocompatibility assessment

Murine fibroblast L-929 and human gingival fibroblast (HGF) cell lines (Zhongqiao Xinzhou Co., Ltd., Shanghai, China) were used to examine the biocompatibility of EGCG-ACP. The cells were cultured in DMEM containing 10% FBS, 100 U/mL penicillin, and 100 μg/mL streptomycin at 37 °C in a 5% $CO_2$ atmosphere. L-929 cell were seeded in a 96-well plate at a density of 5000/well. After 24 h culture, the medium was replaced with a medium containing EGCG-ACP or CPP-ACP (2%) and diluted at 1:1, 1:10, 1:20, 1: 50, or 1:100, as previously reported [20,21]. After 24 h culture, cell viability was detected by CCK-8 assay according to the manufacturer's instructions.

HGFs ($2 \times 10^4$/well) were seeded on the surfaces of cell-climbing films coated with the different solutions and cultured for 24 h [22]. Then, they were rinsed with phosphate-buffered saline, fixed with 4% paraformaldehyde for 10 min, and permeabilized with 0.05% Triton X-100 for 5 min. F-actin and nuclei were stained with fluorescein isothiocyanate–phalloidin (100 nM) and DAPI (10 μg/mL) at room temperature for 30 min and 30 s, respectively. Cell adhesion and extension were observed by CLSM.

### 2.9. Assessment of the in-vivo remineralization efficacy of EGCG-ACP

The in vivo experiment procedure was carried out as described previously [12,19]. Male Sprague-Dawley rats (8 weeks old, ~250 g) were purchased form Zhuhai BesTest Bio-Tech Co., Ltd. (Zhuhai, China), and used to explore the in-vivo remineralization efficiency of EGCG-ACP. All animal procedures were approved by the Institutional Animal Care and Use Committee of Guangzhou Huateng Biomedical Co., Ltd (HTSW221104). At first, all animals were fed with water containing antibiotics (1 g/kg ampicillin) three days to inhibit the growth of inherent bacteria in the mouth. The rats were inoculated continually with *S. mutans* (100 mL, $10^8$ CFU/mL) for 3 days and given food containing 2% sucrose to create a cariogenic environment. Demineralized enamel samples were prepared as described above. Two symmetrical holes were created in each sample for fixation in the rats' oral cavities. After cariogenic model establishment, the samples were placed and treated with deionized water, EGCG, CPP-ACP, and EGCG-ACP, respectively, every 12 h. With the aim of occupying the interproximal space between the maxillary first and second molars, the samples were placed in the rats' mouths and bound with a 0.25-mm stainless-steel ligature wire attached to the maxillary central incisors. They were thus fully exposed to the rat oral cavity. The rats were fed soft food during the experimental period to avoid sample damage. After 14 days, the enamel samples were removed and examined after washing with deionized water.

### 2.10. Statistical analyses

All data are expressed as means ± standard deviations of values from three independent experiments. GraphPad Prism software 8.0 (Boston, MA, USA) was used to analyze the data by independent-sample *t*-test and one-way analysis of variance. The significance level was set to $P < 0.05$. ($^*P < 0.05$, $^{**}P < 0.01$, $^{***}P < 0.001$).

## 3. Results and discussion

### 3.1. EGCG-ACP characteristics

The average EGCG-ACP particle size, determined by DLS, was about 68 nm (Fig. 1A). TEM images confirmed this size and showed that the EGCG-ACP particles were spherical (Fig. 1B). SAED revealed no characteristic dot or ring pattern, indicating that the EGCG-ACP nanocomposite was in the amorphous phase and thus had been synthesized successfully. XPS showed that the nanocomposite was composed of Ca, P, oxygen (O), and carbon (C; Fig. 1C). On the O1s spectrum, EGCG had two main peaks at 531.8 and 533.2 eV, corresponding to the C–OH and C═O groups. The O1s peak representing the C–OH group of EGCG-ACP showed a shift to 532.6 eV; this decrease in the binding energy indicated that phenolic hydroxyl group electron transfer had occurred, confirming the combination of $Ca^{2+}$ with EGCG. On the FTIR spectrum, EGCG had characteristic peaks at 3357, 1461, and 1145 $cm^{-1}$ (Fig. 1D). The forward shift of the stretching vibration peak at 3357 $cm^{-1}$ could be the reason for the partial destruction of hydrogen bonds when EGCG interacted with $Ca^{2+}$ to form the nanocomposite. The in-plane deformation vibration and C–O–H stretching vibration of the phenolic hydroxyl groups were weaker in EGCG-ACP than in EGCG, also reflecting $Ca^{2+}$ binding to EGCG. Though ACP solution is hardly characterized alone, its existence in EGCG-ACP could be identified by the bending vibration peak at 563 $cm^{-1}$, which confirms the combination of EGCG with ACP and the maintenance of the latter's amorphous phase [23,24]. Previous studies have suggested that ACP had a size of approximately 2 nm [13,25]. Nevertheless, these ultrasmall ion clusters themselves are particularly unstable to quickly aggregate and even nucleate. EGCG could serve as a new type of stabilizer to maintain the amorphous phase of ACP, thus inducing enamel repair.

By detecting the amount of $Ca^{2+}$ and $PO_4^{3-}$ released under different pH conditions, we evaluated the stability of EGCG-ACP during changes in the carious microenvironment. EGCG-ACP released ACP slowly under neutral (pH = 7) conditions, reaching cumulative releases of approximately 30% within 4 h and 60% until 24 h (Fig. 1E). Under acidic conditions, the release of ACP was faster and greater overall, reaching 60% within 4 h and >80% within 12 h. These findings suggest that the considerable $H^+$ in acidic saliva competes with $Ca^{2+}$ to bind lone pair electrons on the phenolic hydroxyl groups of EGCG, which accelerates $Ca^{2+}$ dissociation and thereby facilitates the significant burst release of ACP. For the on-demand release of antibacterial drugs and $Ca^{2+}$ and $PO_4^{3-}$ supplementation in the cariogenic environment, the prepared composites needed to be stable at physiological pH and dissolve in an acidic environment [20]. Polyphenols like tannic acid could carry drugs using phenolic hydroxyl groups; for example, tannic acid combined with

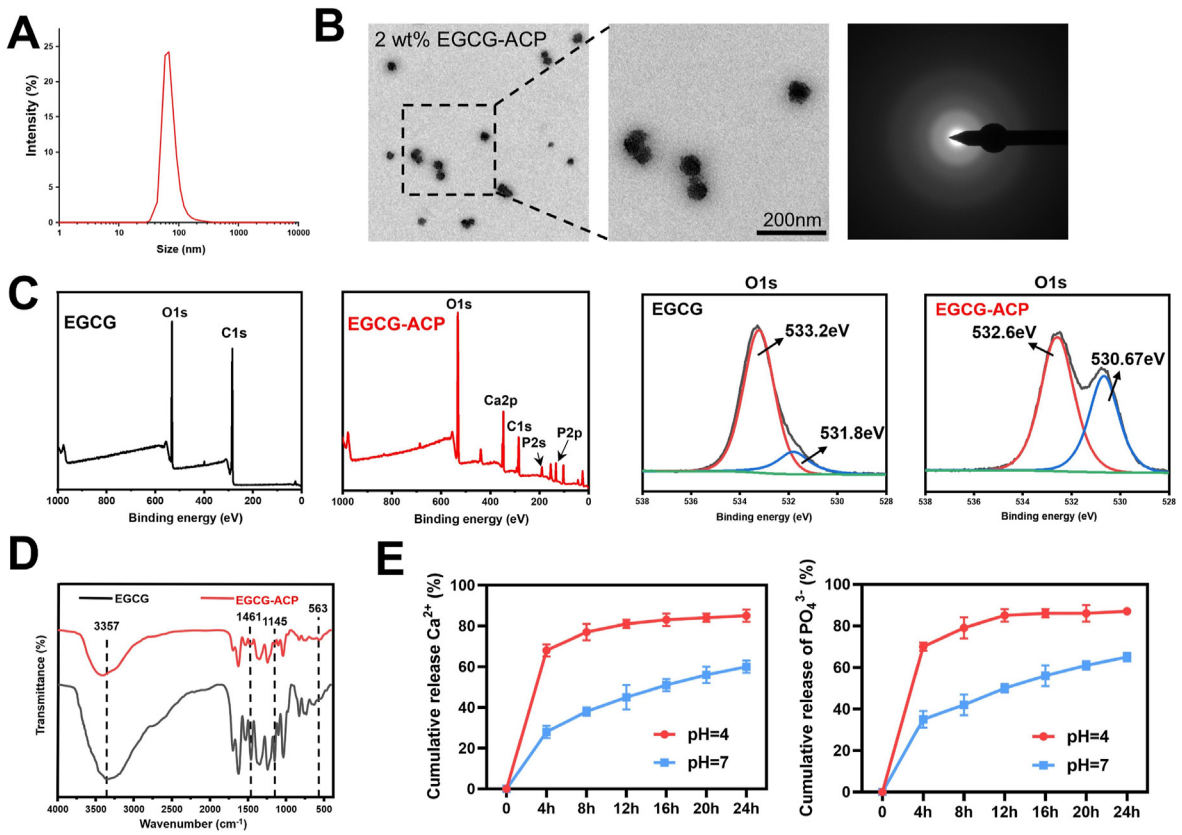


**Fig. 1.** EGCG-ACP nanocomposite (2 wt%) characteristics. (A) DLS size distributions. (B) TEM and SAED images. (C, D) XPS (C) and FTIR (D) spectra of EGCG and EGCG-ACP. (E) Cumulative $Ca^{2+}$ and $PO_4^{3-}$ release from EGCG-ACP in TBS at 37 °C and pH = 7.0 and 4.0.

doxorubicin and infliximab by their hydroxyl groups and released them in response to acidic pH [26,27]. EGCG, as one of the polyphenols, used its phenolic hydroxyl groups to stabilize drugs. Previous studies have demonstrated that EGCG chelated each metal ion with every two phenolic hydroxyl groups and could bind metal ions in a 1:2 ratio [28]. In the EGCG-ACP solution, EGCG interacts with $Ca^{2+}$ to inhibit its combination with $PO_4^{3-}$, thus stabilizing ACP. The pH-responsive release characteristic of EGCG-ACP ensures effective and rapid dissociation in acidic demineralized areas full of cariogenic bacteria, with the release of sufficient EGCG and ACP to exert antibacterial and remineralization effects, respectively [29].

### 3.2. Bioactivity of EGCG-ACP

The biosafety of EGCG-ACP was assessed using CPP-ACP, which has been used safely in clinical practice, as the control. The cell viability, examined by CCK-8 assay, exceeded 80% at dilutions of medium containing EGCG-ACP >1:20, with values similar to those of CPP-ACP (Fig. 2A). These results confirm the excellent biosafety of EGCG-ACP. As gingival contact may occur during EGCG-ACP application, we also evaluated the nanocomposite's effect on HGF morphology. Cytoskeleton staining revealed no ultrastructural change (e.g., cytoskeleton rearrangement or nuclear shrinkage) or over-proliferation of HGFs in the

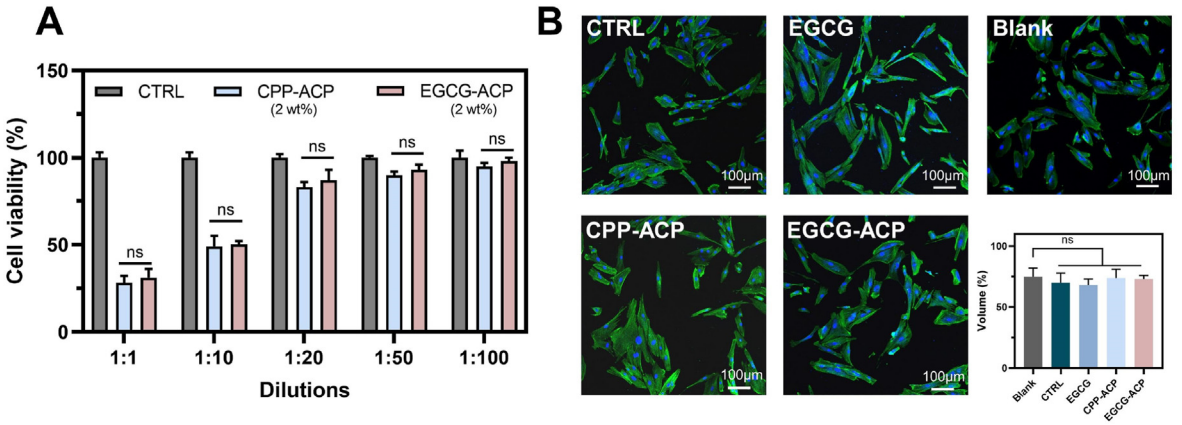


**Fig. 2.** Cytotoxicity assays. (A) Viability of L-929 cells with different dilutions of medium containing EGCG-ACP (2 wt%) or CPP-ACP (2 wt%). Cells exposed to DMEM only were the negative control. (B) Cytoskeleton staining and quantitative fluorescence analysis of HGFs treated with the experimental solutions. Untreated cells served as the blank control.

EGCG-ACP and CPP-ACP groups (Fig. 2B), indicating that the composites did not stimulate gingival hyperplasia. Previous studies indicated that cytoskeleton staining was a more intuitive and vivid method to visualize the cell morphology and activity [20,30]. The quantitative fluorescence analysis showed no significant difference between the control group and the EGCG-ACP group, demonstrating it to be a promising application for clinical transformation. As an active component of natural tea polyphenols, EGCG has good biocompatibility and no toxicity against human dental pulp cells [31]. However, it interferes with cellular physiological reactive oxygen species levels and signal transduction, and its long-term application at high concentration may cause a cellular inflammatory response by inhibiting intracellular antioxidant enzyme synthesis [32,33]. Notably, a small amount of EGCG-ACP was applied to the enamel and the action time was short in this study, avoiding a threat to cell viability.

### 3.3. EGCG-ACP inhibited bacterial proliferation and biofilm formation in vitro

CFU counts indicated the presence of densely distributed *S. mutans* colonies in the control group, the number of which fell to 1 or 0 after treatment with EGCG (up to 99% antibacterial effectiveness; Fig. 3A). In sharp contrast, the antibacterial effectiveness rate for CPP-ACP against ample *S. mutans* colonies, similar to those present in the control group; this poor antibacterial effect is consistent with previous findings [29]. EGCG-ACP had an antibacterial rate of over 85%, which was much higher than that of CPP-ACP. EGCG has been shown to disrupt bacterial membrane integrity via cross-linking with the bacterial phospholipid bilayer through its abundant phenolic hydroxyl groups [34]. Our results showed that the introduction of ACP had little influence on the antibacterial activity of EGCG. A prolonged observation time was also conducted to investigate the long-term efficiency of EGCG-ACP, and the results showed a gradual decrease in its antibacterial effect (Fig. S1). Since the active antibacterial groups in EGCG-ACP would be consumed and gradually decay, its antibacterial effect would decrease with the extension of time [20]. Even so, the antibacterial efficiency of EGCG-ACP was higher than 75% within 3 days and 50% within 7 days. At present, related references investigating the antibacterial activity of EGCG composites usually had observation time within one day [35,36]. It's worth noting that drugs on enamel would be constantly scoured and diluted by saliva; thus, similar drugs were designed to be used every day or twice a day [37,38]. However, CPP-ACP exerted an indirect antibacterial effect by maintaining an environment rich in $Ca^{2+}$ and thereby affecting bacterial endometabolic processes. Turbidimetry performed to further ascertain the antibacterial effect of EGCG-ACP revealed significantly reduced initial OD values with no upward trend over time for the EGCG and EGCG-ACP groups, in contrast to typical S-shaped growth curves for the CPP-ACP groups (Fig. 3B). These results indicate that bacterial growth was stagnant in the former groups, consistent with the CFU counts.

In the examination of effects on *S. mutans* biofilms, control group samples had large areas of dense green fluorescence reflecting vigorous biofilm growth. After CPP-ACP treatment, the amount of biofilm decreased slightly but dead bacteria were rarely observed, indicating the lack of a significant antibiofilm effect [39]. In contrast, almost completely red fluorescence reflecting strong antibiofilm effects was observed on the EGCG and EGCG-ACP samples (Fig. 3C). EGCG inhibits glucosyltransferase activity, hindering bacterial adhesion and plaque biofilm formation [14,40]. Oral cariogenic bacteria present and induce demineralization mainly in biofilm form [41]. Compared with planktonic bacteria, bacterial biofilm tolerates antimicrobial drugs to a certain extent because the extracellular matrix hinders drug penetration [42]. Our results suggest that the introduction of ACP did not significantly influence the bactericidal and antibiofilm abilities of EGCG. Similarly, the chelation of ACP with zwitterionic poly (carboxybetaine acrylamide) did not affect the latter's intrinsic antibacterial ability [12]. Although ACP chelation may weaken the antibacterial properties of EGCG slightly due to the consumption of phenolic hydroxyl groups, the EGCG-ACP nanocomposite exhibited the expected antibacterial efficacy, which would increase further with the gradual dissociation of ACP.

### 3.4. EGCG-ACP promoted remineralization without bacterial interference

SEM showed that the natural enamel surface was smooth and flat, with a few scattered defects. After acid etching, the enamel surface was

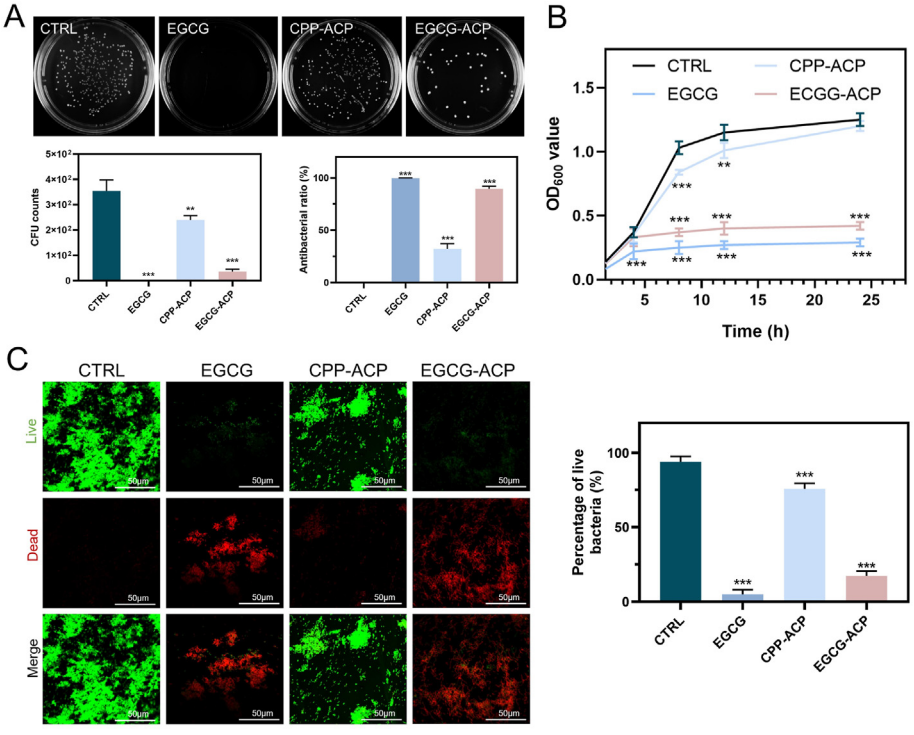


**Fig. 3.** Antibacterial activity. (A) Typical *S. mutans* colonies, CFU counts, and antibacterial ratios. (B) *S. mutans* growth curves. (C) CLSM images of the *S. mutans* biofilm after treatment (green, living cells; red, dead cells) and percentages of viable bacteria in the biofilm. The results represent mean ± SD of three independent experiments. $^{**}P < 0.01$; $^{***}P < 0.001$; compared with control group. (For interpretation of the references to colour in this figure legend, the reader is referred to the Web version of this article.)

rough, and the enamel prisms and glaze sheath left after the dissolution of the glaze sheath around them were clearly visible (Fig. 4A). The tails of the enamel prisms were dissolved slightly more than the heads, resulting in a classic fish-scale structure. In the control group, newly deposited minerals were observed on the enamel surface after immersion in artificial saliva, and deposition increased gradually throughout the immersion cycle. Currently, much work has been done on the outcome of anti-caries products, while the dynamic changes over time was ignored. To investigate the remineralization effect of EGCG-ACP over time, we observed the changes in the enamel specimens in a time-dependent manner. After 7 days of immersion, a thin, porous, uneven layer containing irregularly distributed mineral crystals was present on the enamel surface. The fish-scale morphology remained faintly visible beneath it, indicating that natural remineralization in artificial saliva was insufficient (Fig. 4B). Remineralization in the EGCG group was similar to that in the control group at all timepoints, although shallower pores and loose mineral particle deposition were observed. Mineral crystal formation was slow, probably due to the competitive binding of $Ca^{2+}$ by the phenolic hydroxyl groups in EGCG, resulting in a relative decrease in $Ca^{2+}$ in artificial saliva [43]. Mineralization was faster in the CPP-ACP group, with the formation of a mostly flat surface with a few localized depressions by the 5th day. On the 7th day, the enamel surface was smooth and flat, as the resident HA after acid etching served as a template for ACP nucleation and growth to crystallize and form new HA [13]. The remineralization effect of EGCG-ACP was examined by comparing with CPP-ACP. In the EGCG-ACP group, the newly formed mineral layer was slightly thinner than that in the CPP-ACP group in the early stage (days 1–3), which may be attributed to ACP chelation and uniform release by the functional groups of CPP under neutral conditions. The ACP release rate in the EGCG-ACP group was initially slow and increased gradually, such that the early remineralization effect was inferior to that of CPP-ACP but the final remineralization results were similar. The remineralization effect under sterile conditions reflects the ability of functional drugs to restore demineralized enamel. Both of these composites provided ACP for the initiation of remineralization, which was beneficial for the epitaxial enamel growth induced by the $Ca^{2+}$ and $PO_4^{3-}$ in saliva [13]. On the 7th day, the remineralized layers in the EGCG-ACP group were compact and the microstructure of the regenerated crystals was needle-like with an ordered nanorod structure [44], indicating that the chelated nanoscale ACP particles entered the enamel sheath and provided $Ca^{2+}$ and $PO_4^{3-}$ for remineralization.

EDS analysis indicated that the Ca/P molar ratio of natural enamel was 1.69, close to the stoichiometric standard of HA (1.67), and that this ratio decreased to 1.44 after acid etching (Fig. 4A and B). The Ca/P molar ratios in the control and EGCG groups were 1.50 and 1.48, respectively, and thus only slightly higher than that of the acid-etched samples (Fig. 4C). The CPP-ACP treatment increased the Ca/P molar ratio to 1.80, higher than that of natural enamel due to the large amounts of $Ca^{2+}$ and $PO_4^{3-}$ in the material, which not only promoted enamel restoration but also enabled the mineralization of the most superficial enamel layer, resulting in the excessive accumulation of calcium phosphate [45]. CPP-ACP relies on a single phosphate group to chelate and release ACP,

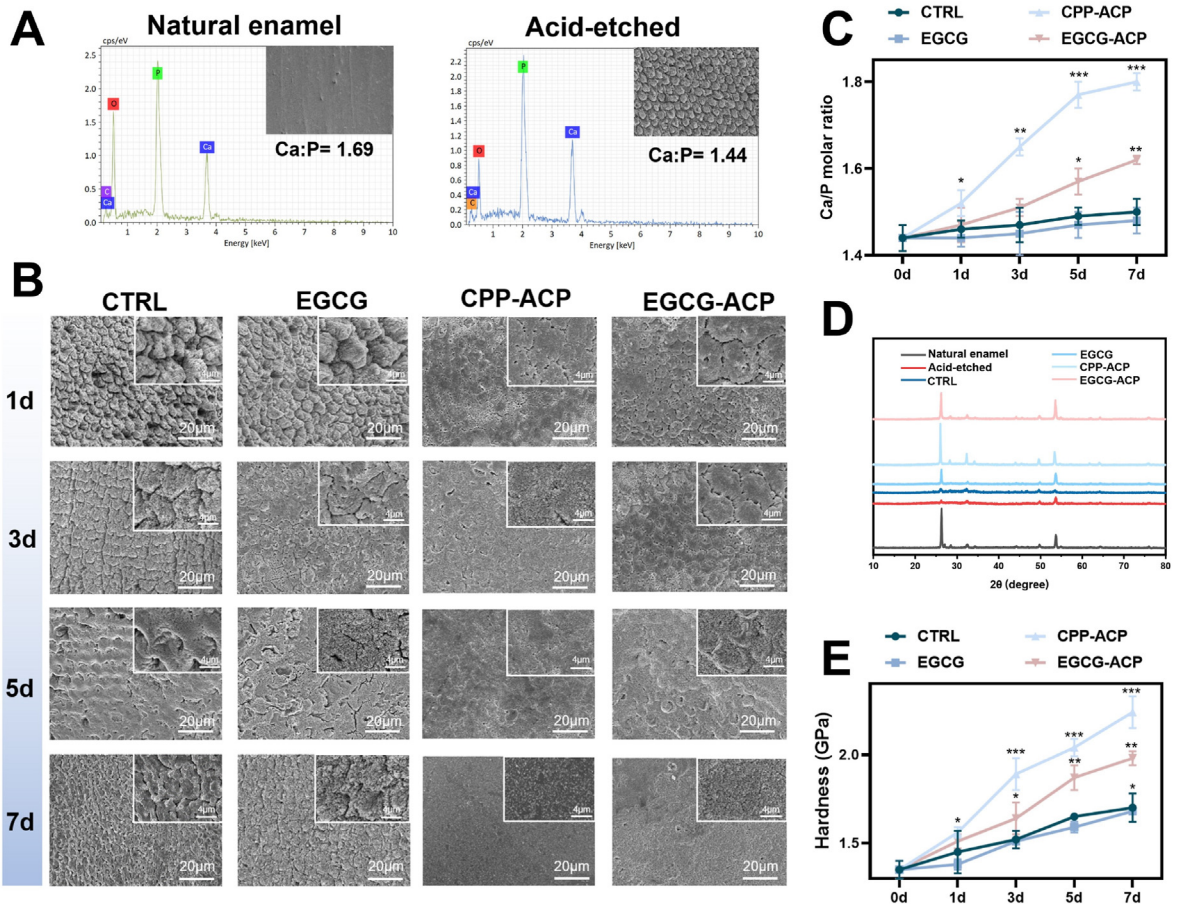


**Fig. 4.** Effects on enamel remineralization under sterile conditions. SEM images and EDS results for natural and demineralized enamel (A), and for demineralized enamel treated with the experimental solutions and immersed in artificial saliva for 1, 3, 5, and 7 days (B). (C) Changes in Ca/P ratio after continuous treatment with the experimental solutions for 7 days. (D) XRD patterns of natural, acid-etched, and demineralized enamel treated with the experimental solutions for 7 days. (E) Changes in demineralized enamel hardness after continuous treatment with the experimental solutions for 7 days. The results represent mean ± SD of three independent experiments. *$P < 0.05$; **$P < 0.01$; ***$P < 0.001$; compared with control group.

while EGCG chelates each ACP with two phenolic hydroxyl groups [28, 29], Thus, the former requires less electrostatic action to overcome to release ACP than the latter, which exerted a higher efficiency to release ACP and the resultant better remineralization effect. Therefore, the hardness of the CPP-ACP group is higher than that of EGCG-ACP. The Ca/P molar ratio in the EGCG-ACP group was 1.62, close to that of natural enamel, which may be related to the slower release of $Ca^{2+}$ and $PO_4^{3-}$ than with CPP-ACP. XRD performed to characterize the enamel crystalline structure showed characteristic HA diffraction peaks in all groups (Fig. 4D), with different relative intensities indicating different crystal orientations [37]. Acid etching markedly weakened or abolished the characteristic (002), (300), (213), and (004) reflection peaks, as a result of HA dissolution in the presence of $H^+$. Little recovery of the characteristic diffraction peaks of the demineralized enamel in the control and EGCG groups was observed, reflecting very limited remineralization ability. After the CPP-ACP and EGCG-ACP treatments, the characteristic (002) peak was similar to that of natural enamel, indicating that newly generated HA had restored the enamel. XRD confirmed that the elevation of Ca/P molar ratios was attributable to HA formation; that is, the newly formed mineral was HA.

The hardness values for natural and acid-etched enamel were 3.04 ± 0.50 and 1.09 ± 0.59 GPa, respectively (Fig. 4E). The control and EGCG groups showed little improvement in enamel hardness. By contrast, the hardness values for the CPP-ACP and EGCG-ACP groups were 1.4–1.6 times higher than that for the control group. Enamel hardness is associated closely with the material's microstructure and chemical composition. After Ca and P dissolution, the remaining organic components (e.g., proteins) have dramatically reduced hardness, impairing the ability of enamel to bear chewing force [46]. Similar to CPP-ACP, EGCG-ACP released ACP to promote orderly Ca and P crystallization and growth, filling the demineralized glaze sheath and thereby restoring the microstructure and mechanical properties of the enamel well. Saturated $Ca^{2+}$ and $PO_4^{3-}$ in bioglass solution have been observed to exert a mineralization regulation effect similar to that of ACP to promote the formation of a remineralization layer [47]. However, such remineralization was disordered and uncontrolled, and thus failed to effectively improve demineralized enamel hardness [47].

### 3.5. EGCG-ACP prevented demineralization in the presence of cariogenic bacteria

Natural enamel samples were immersed in an alternating cycle of acidic bacterial solution (pH = 4, 8 h) and artificial saliva (pH = 7, 4 h) to simulate the presence of oral bacteria and evaluate the protective ability of EGCG-ACP against demineralization. SEM revealed clearly visible enamel prism edges and a fish-scale structure similar to that observed after acid etching in control samples treated for 7 days (Fig. 5A). Cyclic incubation with cariogenic bacteria led to continuous enamel demineralization, and artificial saliva did not prevent this process or promote remineralization. The surface morphology of enamel in the EGCG group was flatter than that in the control group after 1 and 3 days, with fewer pores and defects representing demineralization. Scattered defects and some enamel prism edges were observed after 7 days, suggesting that EGCG killed cariogenic bacteria early and reduced the production of organic acids, delaying the progress of enamel demineralization under bacterial conditions. Significantly less mineral loss had occurred in the EGCG group than in the control group after 7 days, but some loss did occur (Fig. 5B and C), indicating that EGCG could only exert antibacterial effects to reduce demineralization and was unable to promote remineralization [31]. Furthermore, the corresponding results of XRD patterns exhibited characteristic peaks with different intensities, among which the EGCG-ACP group showed the most intense peaks, indicating its anti-demineralization effect (Fig. 5D).

Some mineral deposition with no remarkable demineralization morphology was observed on the enamel surfaces after 3 days of CPP-ACP treatment, and this observation was confirmed by quantitative analysis. However, deep, large, rough cracks formed gradually and the mineral deposition and hardness decreased, indicating a demineralizing tendency. Although CPP-ACP provided the Ca and P required for remineralization, its weak antibacterial property did not prevent the pH

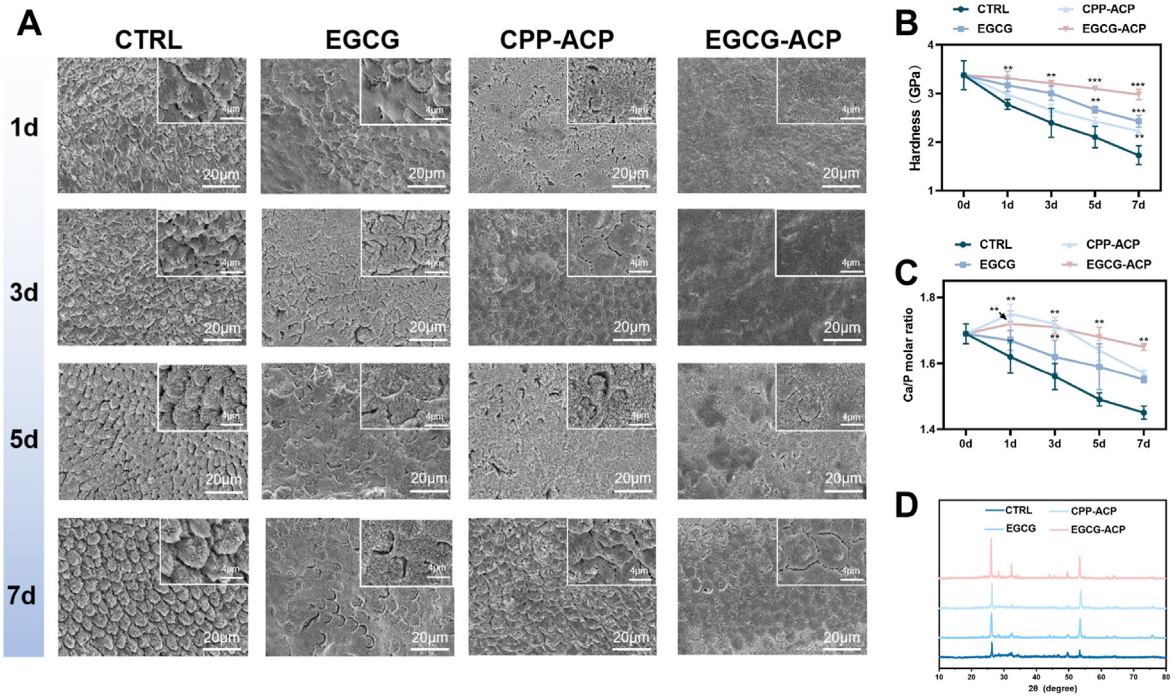


**Fig. 5.** Prevention of enamel demineralization in the presence of cariogenic bacteria. (A) SEM images of natural enamel treated with the experimental solutions and immersed alternately in acidic bacterial solution and artificial saliva for 1, 3, 5, and 7 days. Changes in the hardness (B) and Ca/P ratio (C) of natural enamel treated with the experimental solutions for 7 days. (D) XRD patterns of natural enamel treated with the experimental solutions for 7 days. The results represent mean ± SD of three independent experiments. $^{**}P < 0.01$; $^{***}P < 0.001$; compared with control group.

reduction caused by the acid production of cariogenic bacteria, and it did not confer resistance of the dissolution of unstable minerals in the acidic environment. Thus, CPP-ACP failed to exert the desired preventive effect under bacterial conditions, where $H^+$ continues to penetrate into the deep areas of enamel [12]. The enamel morphology in the EGCG-ACP group was similar to that in the EGCG group on the 1st and 3rd days, and most of the enamel surface remained flat on the 7th day, with occasional demineralization and enamel prism gaps observed. This group showed the least mineral loss and significantly greater hardness than in the other groups, indicating that EGCG-ACP inhibited demineralization development under the interference of cariogenic bacteria. The release of ACP from EGCG-ACP, reflected by the kinetic $Ca^{2+}$ release curve, also was faster at the acidic pH (Fig. 1E), which explains the accelerated dissociation caused by cariogenic bacteria. The protonated EGCG eliminated cariogenic bacteria to provide favorable conditions for remineralization, while the rapid and considerable dissociation of ACP promoted HA crystal formation. Thus, EGCG-ACP had strong antibacterial and remineralization effects in an acidic environment, thereby delaying enamel demineralization and exerting a protective effect.

### 3.6. *In vivo anti-caries and mineralization effects of EGCG-ACP*

In the in-vivo cariogenic model in which demineralized enamel samples were fixed in rat oral cavities (Fig. 6A and B). CFU counts showed that EGCG and EGCG-ACP effectively reduced the bacteria in the in vivo environment (Fig. 6C). The CPP-ACP group exerted certain antibacterial effects while inferior to the EGCG and EGCG-ACP groups. Massive bacteria were observed on the enamel by SEM, especially in the glaze sheath, after 14 days of bacterial inoculation (Fig. 6D). The morphology of the glaze sheath became progressively more pronounced, suggesting that the acid produced by cariogenic bacteria aggravated enamel dissolution. Fewer bacteria adhered to the demineralized enamel, and a thin, uneven layer of mineral deposition was observed, in the EGCG group. These results confirmed that EGCG prevented bacterial enamel destruction, creating favorable conditions for the deposition of Ca and P from saliva. In the CPP-ACP group, a mass of bacteria adhered to the demineralized area and a small number of remineralized crystals formed in the area without bacterial colonization. In sharp contrast, the regenerated mineral layer on the enamel surface in the EGCG-ACP group was more even and uniform, with fewer adhering bacteria. The EGCG-ACP group had a markedly higher hardness and Ca/P ratio than all other groups (Fig. 6E and F), which revealed the most remineralization ability and restoration of the mechanical strength of the enamel structure. The XRD results were consistent with the SEM images, which showed that crystalline structures after remineralization by EGCG-ACP were more closely resembled to the normal enamel (Fig. 6G). These findings indicated that EGCG-ACP enhanced the restoration of demineralized enamel in vivo through two underlying mechanisms: (i) the inhibition of cariogenic bacterial proliferation and biofilm development via EGCG release to prevent the progression of caries, and (ii) the promotion of enamel remineralization via ACP release. The in vivo results reflected the clinical potential of EGCG-ACP for the effective treatment of dental caries

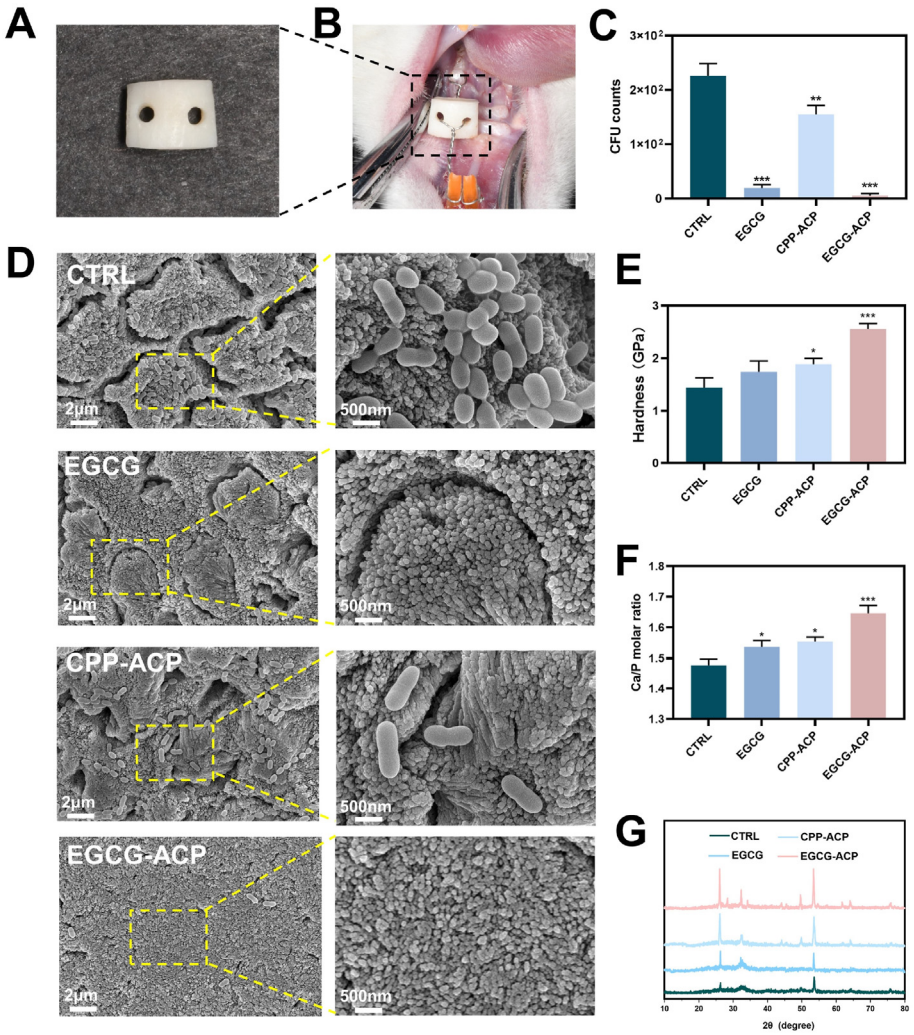


**Fig. 6.** In vivo enamel remineralization in rats. (A) Perforated enamel samples. (B) Fixation of demineralized enamel samples in the rat oral cavity. (C) Quantitative data of CFU in vivo. (D–F) SEM images (D), changes in the hardness (E), and Ca/P ratio (F) of enamel samples treated with the experimental materials after 14 days of incubation in rat oral cavities inoculated with *S. mutans*. (G) XRD patterns of enamel samples treated with the experimental materials after 14 days in vivo. The results represent mean ± SD of three independent experiments. $^*P < 0.05$; $^{**}P < 0.01$; $^{***}P < 0.001$; compared with control group.

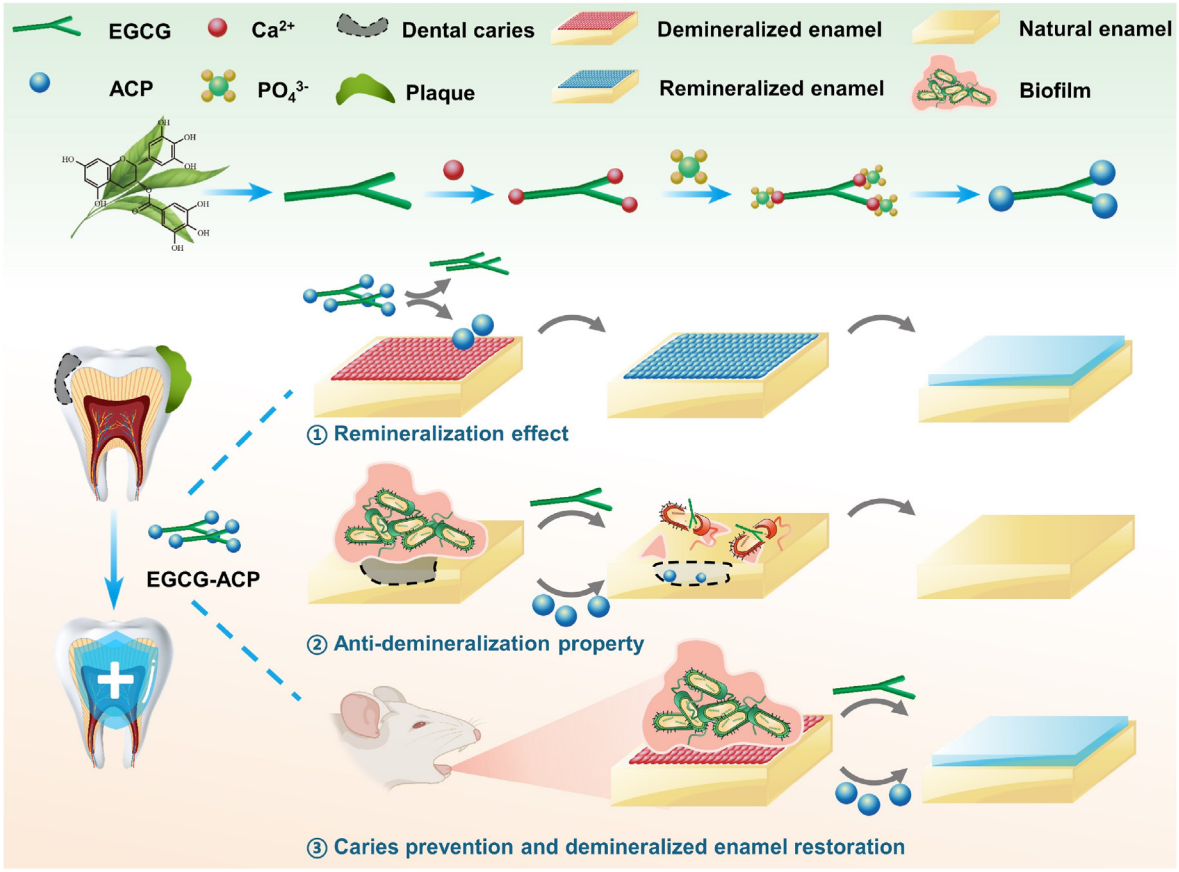


**Fig. 7.** Schematic illustration of EGCG-ACP's promotion of enamel remineralization and prevention of demineralization in vitro, and its restoration of enamel remineralization in the presence of bacteria in vivo.

through simple mouth washing or smearing. People could rinse the mouth for at-home treatment to obtain a desired remineralization efficiency. By creating an optimized scheme, the remineralization efficiency by EGCG-ACP can be further improved. For example, since EGCG-ACP could be applied to initiate the growth of crystals on enamel, a following extra supply of sufficient source of calcium and phosphate ion may further promote the remineralization process [19]. In addition, applying EGCG-ACP before placing the adhesive and resin to fill enamel defects may inhibit the bacterial influence and establish a biomimetic mineralization frontier for remineralization, which is beneficial for a stable resin-dentin bonded interface [37]. However, further investigation is required to determine whether the organic components of EGCG-ACP would leave over and affect the bonding strength of the adhesive and resin composites.

In summary, the findings of this study indicate that CPP-ACP promotes remineralization under sterile conditions, but has a poor ability to prevent demineralization and promote remineralization under bacterial conditions. EGCG did not significantly promote remineralization, but delayed demineralization by inhibiting bacteria. EGCG-ACP promoted remineralization by providing ACP, which was accelerated under acidic conditions due to the rapid dissociation of EGCG and ACP. The dissociated EGCG exerted antibacterial effects to create a supportive environment for remineralization by ACP, which not only prevents enamel demineralization but also promotes enamel restoration in a cariogenic environment. These results indicate that EGCG-ACP has a prospective application to prevent enamel demineralization in patients with high caries risk. A limitation of this study is that all experiments were performed at 37 °C; the temperature in the oral cavity, in contrast, changes dynamically during eating and other physiological activities [48]. Whether temperature influences the antibacterial and remineralization effects of EGCG-ACP needs to be explored. In addition, as oral bacteria survive in the form of flora ecosystems [49,50], additional research is needed to determine whether EGCG-ACP affects the diversity and ecological balance of the oral flora, and to examine its long-term effects and feasibility of use.

## 4. Conclusion

In this study, an EGCG-ACP nanocomposite was formed successfully by using EGCG to stabilize $Ca^{2+}$ and $PO_4^{3-}$, and it was demonstrated to protect enamel and promote remineralization. EGCG compounded with ACP retained its ability to inhibit *S. mutans* proliferation and biofilm formation, thereby effectively preventing the development of demineralization. In vitro, the remineralization effects of EGCG-ACP were similar to those of CPP-ACP under sterile conditions to restore the demineralized enamel. Under simulated bacterial acid production, EGCG-ACP dissociated rapidly and released EGCG to exert antibacterial effects and delay the progression of demineralization to prevent caries, which was further confirmed by in-vivo results (Fig. 7). The rapid release of ACP enabled rapid enamel remineralization and protected demineralized enamel from caries progression. The mechanical properties of the regenerated mineral layer were equivalent to those of natural enamel. Thus, EGCG-ACP application improves the degree of mineralization and mechanical properties of regenerated enamel, and is a promising alternative therapy to achieve the partial restoration of demineralized enamel, and prevent the occurrence and development of tooth erosion and caries.

## Credit author statement

**Danni Dai**: Methodology, Data curation, Investigation, Visualization,

Writing - Original Draft, Writing - review & editing. **Jianrong Wang**: Investigation, Validation. **Hanshu Xie:** Investigation, Validation. **Chao Zhang**: Conceptualization, Supervision, Writing - Original Draft, Writing - review & editing, Funding acquisition.

## Declaration of competing interest

The authors declare that they have no known competing financial interests or personal relationships that could have appeared to influence the work reported in this paper.

## Data availability

Data will be made available on request.

## Acknowledgments

This work was supported by the National Natural Science Foundation of China (81801007); the Natural Science Foundation of Guangdong Province (2018A030310442); the Major of Basic and Applied Basic Research Project of Guangzhou City (202201011601); and the Science and Cultivation Foundation of Stomatological Hospital of Southern Medical University (PY2021016).

## Appendix A. Supplementary data

Supplementary data to this article can be found online at https://doi.org/10.1016/j.mtbio.2023.100715.

## References

[1] L. Cheng, L. Zhang, L. Yue, J. Ling, M. Fan, D. Yang, Z. Huang, Y. Niu, J. Liu, J. Zhao, Y. Li, B. Guo, Z. Chen, X. Zhou, Expert consensus on dental caries management, Int. J. Oral Sci. 14 (1) (2022) 17, https://doi.org/10.1038/s41368-022-00167-3.

[2] A.D. Anastasiou, S. Strafford, C.L. Thomson, J. Gardy, T.J. Edwards, M. Malinowski, S.A. Hussain, N.K. Metzger, A. Hassanpour, C.T.A. Brown, A.P. Brown, M.S. Duggal, A. Jha, Exogenous mineralization of hard tissues using photo-absorptive minerals and femto-second lasers; the case of dental enamel, Acta Biomater. 71 (2018) 86–95, https://doi.org/10.1016/j.actbio.2018.02.012.

[3] D. Wang, M. Haapasalo, Y. Gao, J. Ma, Y. Shen, Antibiofilm peptides against biofilms on titanium and hydroxyapatite surfaces, Bioact. Mater. 3 (4) (2018) 418–425, https://doi.org/10.1016/j.bioactmat.2018.06.002.

[4] P. Sorkhdini, R.L. Gregory, Y.O. Crystal, Q. Tang, F. Lippert, Effectiveness of in vitro primary coronal caries prevention with silver diamine fluoride - chemical vs biofilm models, J. Dent. 99 (2020), 103418, https://doi.org/10.1016/j.jdent.2020.103418.

[5] M. Schneider-Rayman, D. Steinberg, R.V. Sionov, M. Friedman, M. Shalish, Effect of epigallocatechin gallate on dental biofilm of Streptococcus mutans: an in vitro study, BMC Oral Health 21 (1) (2021) 447, https://doi.org/10.1186/s12903-021-01798-4.

[6] W.C. Reygaert, The antimicrobial possibilities of green tea, Front. Microbiol. 5 (2014) 434, https://doi.org/10.3389/fmicb.2014.00434.

[7] G.M. Lee, S.-j. Kim, E.M. Kim, E. Kim, S. Lee, E. Lee, H.H. Park, H. Shin, Free radical-scavenging composite gelatin methacryloyl hydrogels for cell encapsulation, Acta Biomater. 149 (2022) 96–110, https://doi.org/10.1016/j.actbio.2022.06.043.

[8] M. Farhan, Green tea catechins: nature's way of preventing and treating cancer, Int. J. Mol. Sci. 23 (18) (2022), 10713, https://doi.org/10.3390/ijms231810713.

[9] J. Duan, Z. Chen, X. Liang, Y. Chen, H. Li, X. Tian, M. Zhang, X. Wang, H. Sun, D. Kong, Y. Li, J. Yang, Construction and application of therapeutic metal-polyphenol capsule for peripheral artery disease, Biomaterials 255 (2020), 120199, https://doi.org/10.1016/j.biomaterials.2020.120199.

[10] L. Yi, H. Wu, Y. Xu, J. Yu, Y. Zhao, H. Yang, C. Huang, Biomineralization-inspired sandwich dentin desensitization strategy based on multifunctional nanocomposite with yolk-shell structure, Nanoscale 15 (1) (2022) 127–143, https://doi.org/10.1039/d2nr04993g.

[11] J. Yan, H. Yang, T. Luo, F. Hua, H. He, Application of amorphous calcium phosphate agents in the prevention and treatment of enamel demineralization, Front. Bioeng. Biotechnol. 10 (2022), 853436, https://doi.org/10.3389/fbioe.2022.853436.

[12] J. He, J. Yang, M. Li, Y. Li, Y. Pang, J. Deng, X. Zhang, W. Liu, Polyzwitterion manipulates remineralization and antibiofilm functions against dental demineralization, ACS Nano 16 (2) (2022) 3119–3134, https://doi.org/10.1021/acsnano.1c10812.

[13] C. Shao, B. Jin, Z. Mu, H. Lu, Y. Zhao, Z. Wu, L. Yan, Z. Zhang, Y. Zhou, H. Pan, Z. Liu, R. Tang, Repair of tooth enamel by a biomimetic mineralization frontier ensuring epitaxial growth, Sci. Adv. 5 (8) (2019), eaaw9569, https://doi.org/10.1126/sciadv.aaw9569.

[14] J. Li, X. Xie, Y. Wang, W. Yin, J.S. Antoun, M. Farella, L. Mei, Long-term remineralizing effect of casein phosphopeptide-amorphous calcium phosphate (CPP-ACP) on early caries lesions in vivo: a systematic review, J. Dent. 42 (7) (2014) 769–777, https://doi.org/10.1016/j.jdent.2014.03.015.

[15] F. Heravi, H. Bagheri, A. Rangrazi, S.M. Zebarjad, Effects of the addition of casein phosphopeptide-amorphous calcium phosphate (CPP-ACP) on mechanical properties of luting and lining glass ionomer cement, Mater. Res. Express 3 (7) (2016), 075405, https://doi.org/10.1088/2053-1591/3/7/075405.

[16] E.C. Reynolds, F. Cai, N.J. Cochrane, P. Shen, G.D. Walker, M.V. Morgan, C. Reynolds, Fluoride and casein phosphopeptide-amorphous calcium phosphate, J. Dent. Res. 87 (4) (2008) 344–348, https://doi.org/10.1177/154405910808700420.

[17] H.B. Dias, M.I.B. Bernardi, V.S. Marangoni, A.C. de Abreu Bernardi, A.N. de Souza Rastelli, A.C. Hernandes, Synthesis, characterization and application of Ag doped ZnO nanoparticles, in a composite resin, Mater. Sci. Eng. C Mater. Biolog. App. 96 (2019) 391–401, https://doi.org/10.1016/j.msec.2018.10.063.

[18] M. Mao, W. Zhang, Z. Huang, J. Huang, J. Wang, W. Li, S. Gu, Graphene oxide-copper nanocomposites suppress cariogenic Streptococcus mutans biofilm formation, Int. J. Nanomed. 16 (2021) 7727–7739, https://doi.org/10.2147/ijn.S303521.

[19] D. Wang, J. Deng, X. Deng, C. Fang, X. Zhang, P. Yang, Controlling enamel remineralization by amyloid-like amelogenin mimics, Adv. Mater. 32 (31) (2020), e2002080, https://doi.org/10.1002/adma.202002080.

[20] Y. Xu, Y. You, L. Yi, X. Wu, Y. Zhao, J. Yu, H. Liu, Y. Shen, J. Guo, C. Huang, Dental plaque-inspired versatile nanosystem for caries prevention and tooth restoration, Bioact. Mater. 20 (2023) 418–433, https://doi.org/10.1016/j.bioactmat.2022.06.010.

[21] G. Bhadila, X. Wang, W. Zhou, D. Menon, M.A.S. Melo, S. Montaner, T.W. Oates, M.D. Weir, J. Sun, H.H.K. Xu, Novel low-shrinkage-stress nanocomposite with remineralization and antibacterial abilities to protect marginal enamel under biofilm, J. Dent. 99 (2020), 103406, https://doi.org/10.1016/j.jdent.2020.103406.

[22] R. Fontelo, D.S. da Costa, M. Gomez-Florit, H. Tiainen, R.L. Reis, R. Novoa-Carballal, I. Pashkuleva, Antibacterial nanopatterned coatings for dental implants, J. Mater. Chem. B 10 (42) (2022) 8710–8718, https://doi.org/10.1039/d2tb01352e.

[23] L. Kind, S. Stevanovic, S. Wuttig, S. Wimberger, J. Hofer, B. Mueller, U. Pieles, Biomimetic remineralization of carious lesions by self-assembling peptide, J. Dent. Res. 96 (7) (2017) 790–797, https://doi.org/10.1177/0022034517698419.

[24] X. Lu, Y. Qu, T. Zhu, X. Qu, Z. Zhang, Y. Yu, Y. Hao, Applications of photothermally mediated nanohybrids for white spot lesions in orthodontics, Colloids Surf. B Biointerfaces 225 (2023) 113274, https://doi.org/10.1016/j.colsurfb.2023.113274, 113274.

[25] H. Yu, N.-w. Jiang, X.-y. Ye, H.-y. Zheng, T. Attin, H. Cheng, In situ effect of Tooth Mousse containing CPP-ACP on human enamel subjected to in vivo acid attacks, J. Dent. 76 (2018) 40–45, https://doi.org/10.1016/j.jdent.2018.05.021.

[26] M. Haktaniyan, S. Atilla, E. Cagli, I. Erel-Goktepe, pH- and temperature-induced release of doxorubicin from multilayers of poly(2-isopropyl-2-oxazoline) and tannic acid, Polym. Int. 66 (12) (2017) 1851–1863, https://doi.org/10.1002/pi.5458.

[27] X. Wang, J. Yan, L. Wang, D. Pan, Y. Xu, F. Wang, J. Sheng, X. Li, M. Yang, Oral delivery of anti-TNF antibody shielded by natural polyphenol-mediated supramolecular assembly for inflammatory bowel disease therapy, Theranostics 10 (23) (2020) 10808–10822, https://doi.org/10.7150/thno.47601.

[28] L.-m. Sun, C.-l. Zhang, P. Li, Characterization, antimicrobial activity, and mechanism of a high-performance (-)-Epigallocatechin-3-gallate (EGCG)-Cu-II/Polyvinyl alcohol (PVA) nanofibrous membrane, J. Agric. Food Chem. 59 (9) (2011) 5087–5092, https://doi.org/10.1021/jf200580t.

[29] P. Shen, J.R. Fernando, G.D. Walker, Y. Yuan, C. Reynolds, E.C. Reynolds, Addition of CPP-ACP to yogurt inhibits enamel subsurface demineralization, J. Dent. 103 (2020), 103506, https://doi.org/10.1016/j.jdent.2020.103506.

[30] M.P. Pecci-Lloret, S. Lopez-Garcia, F.J. Rodriguez-Lozano, P. Alvarez-Novoa, D. Garcia-Bernal, In vitro biocompatibility of several children's toothpastes on human gingival fibroblasts, Int. J. Environ. Res. Publ. Health 19 (5) (2022) 2954, https://doi.org/10.3390/ijerph19052954.

[31] J. Yu, L. Yi, R. Guo, J. Guo, H. Yang, C. Huang, The stability of dentin surface biobarrier consisting of mesoporous delivery system on dentinal tubule occlusion and Streptococcus mutans biofilm inhibition, Int. J. Nanomed. 16 (2021) 3041–3057, https://doi.org/10.2147/ijn.S290254.

[32] M. Panji, V. Behmard, Z. Zare, M. Malekpour, H. Nejadbiglari, S. Yavari, T.N. Dizaj, A. Safaeian, N. Maleki, M. Abbasi, O. Abazari, M. Shabanzadeh, P. Khanicheragh, Suppressing effects of green tea extract and Epigallocatechin-3-gallate (EGCG) on TGF-beta- induced Epithelial-to-mesenchymal transition via ROS/Smad signaling in human cervical cancer cells, Gene 794 (2021), 145774, https://doi.org/10.1016/j.gene.2021.145774.

[33] D. Wang, Y. Wang, X. Wan, C.S. Yang, J. Zhang, Green tea polyphenol (-)-epigallocatechin-3-gallate triggered hepatotoxicity in mice: responses of major antioxidant enzymes and the Nrf2 rescue pathway, Toxicol. Appl. Pharmacol. 283 (1) (2015) 65–74, https://doi.org/10.1016/j.taap.2014.12.018.

[34] Y. Asahi, Y. Noiri, J. Miura, H. Maezono, M. Yamaguchi, R. Yamamoto, H. Azakami, M. Hayashi, S. Ebisu, Effects of the tea catechin epigallocatechin gallate on Porphyromonas gingivalis biofilms, J. Appl. Microbiol. 116 (5) (2014) 1164–1171, https://doi.org/10.1111/jam.12458.

[35] S. Xu, L. Chang, Y. Hu, X. Zhao, S. Huang, Z. Chen, X. Ren, X. Mei, Tea polyphenol modified, photothermal responsive and ROS generative black phosphorus quantum dots as nanoplatforms for promoting MRSA infected wounds healing in diabetic rats, J. Nanobiotechnol. 19 (1) (2021) 362, https://doi.org/10.1186/s12951-021-01106-w.

[36] X. Zhang, J. He, L. Qiao, Z. Wang, Q. Zheng, C. Xiong, H. Yang, K. Li, C. Lu, S. Li, H. Chen, X. Hu, 3D printed PCLA scaffold with nano-hydroxyapatite coating doped green tea EGCG promotes bone growth and inhibits multidrug-resistant bacteria colonization, Cell Prolif. 55 (10) (2022), e13289, https://doi.org/10.1111/cpr.13289.

[37] K. Liang, S. Wang, S. Tao, S. Xiao, H. Zhou, P. Wang, L. Cheng, X. Zhou, M.D. Weir, T.W. Oates, J. Li, H.H.K. Xu, Dental remineralization via poly(amido amine) and restorative materials containing calcium phosphate nanoparticles, Int. J. Oral Sci. 11 (2019) 15, https://doi.org/10.1038/s41368-019-0048-z.

[38] M. Malinowski, K.J. Toumba, S.M. Strafford, M.S. Duggal, The effect on dental enamel of the frequency of consumption of fluoridated milk with a cariogenic challenge in situ, J. Dent. 70 (2018) 87–91, https://doi.org/10.1016/j.jdent.2017.12.016.

[39] S.G. Dashper, P. Shen, C.P.C. Sim, S.W. Liu, C.A. Butler, H.L. Mitchell, T. D'Cruze, Y. Yuan, B. Hoffmann, G.D. Walker, D.V. Catmull, C. Reynolds, E.C. Reynolds, CPP-ACP promotes SnF2 efficacy in a polymicrobial caries model, J. Dent. Res. 98 (2) (2019) 218–224, https://doi.org/10.1177/0022034518809088.

[40] C.-Y. Wu, T.-Y. Su, M.-Y. Wang, S.-F. Yang, K. Mar, S.-L. Hung, Inhibitory effects of tea catechin epigallocatechin-3-gallate against biofilms formed from Streptococcus mutans and a probiotic lactobacillus strain, Arch. Oral Biol. 94 (2018) 69–77, https://doi.org/10.1016/j.archoralbio.2018.06.019.

[41] W.H. Bowen, R.A. Burne, H. Wu, H. Koo, Oral biofilms: pathogens, matrix, and polymicrobial interactions in microenvironments, Trends Microbiol. 26 (3) (2018) 229–242, https://doi.org/10.1016/j.tim.2017.09.008.

[42] Y. Jiao, F.R. Tay, L.-n. Niu, J.-h. Chen, Advancing antimicrobial strategies for managing oral biofilm infections, Int. J. Oral Sci. 11 (2019) 28, https://doi.org/10.1038/s41368-019-0062-1.

[43] V. Carnovale, T. Huppertz, M. Britten, L. Bazinet, Impact of calcium on the interactions between epigallocatechin-3-gallate and alpha(S1)-casein, Int. Dairy J. 102 (2020), 104608, https://doi.org/10.1016/j.idairyj.2019.104608.

[44] A. Hou, J. Luo, M. Zhang, J. Li, W. Chu, K. Liang, J. Yang, J. Li, Two-in-one strategy: a remineralizing and anti-adhesive coating against demineralized enamel, Int. J. Oral Sci. 12 (1) (2020) 27, https://doi.org/10.1038/s41368-020-00097-y.

[45] N.L. Huq, H. Myroforidis, K.J. Cross, D.P. Stanton, P.D. Veith, B.R. Ward, E.C. Reynolds, The interactions of CPP-ACP with saliva, Int. J. Mol. Sci. 17 (6) (2016) 915, https://doi.org/10.3390/ijms17060915.

[46] Y. Bai, Z. Yu, L. Ackerman, Y. Zhang, J. Bonde, W. Li, Y. Cheng, S. Habelitz, Protein nanoribbons template enamel mineralization, Proc. Natl. Acad. Sci. U.S.A. 117 (32) (2020) 19201–19208, https://doi.org/10.1073/pnas.2007838117.

[47] N. Jafari, M.S. Habashi, A. Hashemi, R. Shirazi, N. Tanideh, A. Tamadon, Application of bioactive glasses in various dental fields, Biomater. Res. 26 (1) (2022) 31, https://doi.org/10.1186/s40824-022-00274-6.

[48] R.J. Lamont, H. Koo, G. Hajishengallis, The oral microbiota: dynamic communities and host interactions, Nat. Rev. Microbiol. 16 (12) (2018) 745–759, https://doi.org/10.1038/s41579-018-0089-x.

[49] X. Peng, L. Cheng, Y. You, C. Tang, B. Ren, Y. Li, X. Xu, X. Zhou, Oral microbiota in human systematic diseases, Int. J. Oral Sci. 14 (1) (2022) 14, https://doi.org/10.1038/s41368-022-00163-7.

[50] L. Gao, T. Xu, G. Huang, S. Jiang, Y. Gu, F. Chen, Oral microbiomes: more and more importance in oral cavity and whole body, Protein Cell 9 (5) (2018) 488–500, https://doi.org/10.1007/s13238-018-0548-1.